ELSEVIER

Catalysis Today 81 (2003) 337–345

CATALYSIS TODAY

www.elsevier.com/locate/cattod

Fundamental insights into the oxidative dehydrogenation of ethane to ethylene over catalytic materials discovered by an evolutionary approach

G. Grubert [a,*], E. Kondratenko [a], S. Kolf [a], M. Baerns [a], P. van Geem [b], R. Parton [b]

[a] *Institute for Applied Chemistry Berlin-Adlershof e.V., Richard-Willstätter Street 12, 12489 Berlin, Germany*
[b] *DSM Research, P.O. Box 18, 6160 MD Geleen, The Netherlands*

Received 2 June 2002; received in revised form 6 December 2002; accepted 8 January 2003

Abstract

An evolutionary optimisation procedure combined with high-throughput synthesis and testing has been applied for discovering new catalytic materials for the oxidative dehydrogenation of ethane to ethylene (ODHE). After 10 generations comprising a total of 600 vanadium-free catalytic compositions supported on α-Al_2O_3, Cr/Co/Sn/W and Cr/Mo mixed oxides have been identified as new well performing catalytic materials for the ODHE reaction; ethylene yields of up to 20% and selectivities of 55–65% (500 °C; C_2H_6:O_2:Ar = 20:10:70) were achieved.

The surface and bulk characteristics of the new catalytic materials derived from near-surface composition, binding energies of the elements (XPS), and phase analysis (XRD) as well as from their surface area (BET) lead to the assumption that for both systems (Cr/Mo or Co/Cr/Sn/W oxide) the active phase is located in the X-ray amorphous part of the material. Based on transient and isotopic experiments it was concluded that the ODHE reaction follows the Mars–Van Krevelen mechanism. The different selectivities towards CO_2 and CO between the two systems have been attributed to parallel and consecutive reaction schemes of the product formation, derived from transient experiments. From the fundamental insights obtained improvements of the catalytic performance in the ODHE reaction are suggested.

Keywords: Oxidative dehydrogenation; High-throughput synthesis and testing; Evolutionary approach; Transient study

1. Introduction

The oxidative dehydrogenation of ethane to ethylene (ODHE) has attracted a growing interest during the last decade since it may present an alternative to the highly endothermic thermal pyrolysis [1]. Different reaction conditions have been investigated comprising: (i) easily reducible metal oxide catalysts within a low-temperature range between 300 and 500 °C and contact times from 0.1 to 10 s [2]; and (ii) platinum [3,4] or rare-earth metal oxide catalysts [5] within a high-temperature range between 750 and 1000 °C at millisecond contact times. For the low-temperature conditions, mainly vanadium containing catalysts were identified as best performing materials and their ethylene yields did not exceed 30–40% [6]. In the high-temperature range catalyst-assisted homogenous gas-phase reactions generally play an important role

* Corresponding author. Tel.: +49-306392-4412/4108.
E-mail address: grubert@aca-berlin.de (G. Grubert).

0920-5861/03/$ – see front matter © 2003 Elsevier B.V. All rights reserved.
doi:10.1016/S0920-5861(03)00132-9

and ethylene yields of up to 60% are obtained. From an industrial point of view, ethylene yields between 65 and 70% are required to compete with the steam cracking process. The aim of the present contribution is to illustrate the application of an evolutionary approach [7,8] for the search of new vanadium-free catalytic materials for the ODHE reaction in the low-temperature range. A further characterisation of the new well performing materials shall reveal insights into the active phase and the reaction mechanism, which might lead to a new working hypothesis for improved catalytic compositions or reaction operation as has been shown in a previous study [9].

2. Methodology and experimental

2.1. Evolutionary approach

For the evolutionary optimisation strategy each generation comprises 60 individual catalytic materials. Each material of the first generation was prepared by randomly choosing three elements and their amounts from a pool of 13 elements. The compositions within the following generations were derived by an evolutionary procedure, applying mutation and crossover operators taking into account the objective function, i.e. the ethylene yield under standard condition of the preceding generations. The pool of elements has been chosen on the basis of fundamental knowledge [2,10,11] and is listed in Table 1. In order to discover a new class of active materials, elements with a known catalytic activity like vanadium were replaced by other elements, whose mixtures have not been considered for this reaction until now. Halides have been intentionally excluded because of their possibility to leach into the product gas and cause corrosion, emission of halogenated compounds, and poisoning of catalysts in subsequent processes, like selective hydrogenations or ethylene polymerisation.

2.2. Materials synthesis and testing

The catalytic materials were prepared using a Sophas Synthesis Robot (Zinsser). In the preparation procedure metal salt precursors were deposited on α-Al_2O_3 spheres (Condea, BET 5 m^2/g; d_p = 250–355 μm). The total mass of each individual catalytic material amounted to about 1.25 g. Twenty weight percent corresponds to the active components which were mainly deposited as an eggshell around the support. After calcination (air/350 °C/12 h), 200 mg of each material were tested for the ODHE reaction in a 64-channel fixed-bed continuous flow reactor, under standard conditions (500 °C; C_2H_6:O_2:Ar = 20:10:70; τ = 0.4 g s/ml; 1 bar). Some materials were calcined at temperatures between 350 and 600 °C. In order to find the optimum conditions for the individual catalytic materials the reaction temperature and the contact time were varied between 300 and 500 °C and 0.1–1 g s/ml, respectively. Details of the accelerated synthesis and testing procedure have been reported earlier [12].

2.3. Materials characterisation

Specific surface areas of the materials were determined by the one-point BET method (Gemini III Micromeritics). XRD powder analysis was carried out using a STADIP transmission powder diffractometer (Stoe) with Cu Kα1 radiation. The near-surface composition of the catalytic materials and binding energies of the metal ions were derived from XPS spectra (ESCALAB 220i-XL, Fisons Instruments) using Al Kα radiation (1486.6 eV).

Table 1
Selection of the pool of elements excluding vanadium and chlorines for the evolutionary approach from fundamental knowledge

Assumed mechanism	Required property of active phase	Metal oxide[a] [17,21,23]
Participation of removable lattice oxygen (redox-type catalysts)	Redox properties: medium O–Me binding energy	Cr_2O_3, CuO, MnO_2, MoO_3, WO_3, Ga_2O_3, CoO, SnO_2
Activation by adsorbed oxygen	Dissociative adsorption of oxygen	CaO, La_2O_3
Activation by lattice oxygen	High O–Me binding energy	ZrO_2

[a] Dopants: P and Au (in traces).

For a more detailed understanding of the reaction mechanism transient experiments were carried out in the TAP-2 reactor system. Information on the reactor system is described in [13]. In the TAP reactor the catalytic material (30–140 mg; d_p = 250–355 μm) was placed between two layers of quartz of the same particle size. The transient experiments were carried out at different temperatures between 350 and 500 °C. One pulse consists of 10^{14}–5×10^{14} molecules.

Before each experiment the catalyst was treated in a flow of O_2 (30 ml/min) at 350 °C and ambient pressure for ca. 1 h. Then the reactor was evacuated for 20 min at 350 °C to a final pressure of ca. 10^{-4} Pa. After the vacuum treatment the temperature of the catalyst was set to the desired value. Two types of transient experiments were carried out:

- Gas mixtures of a certain composition (C_2H_6:Ne = 1:1, C_2H_4:Ne = 1:1, CO:Ne = 1:1 and CO_2:Ne = 1:1) were pulsed into the reactor and transient responses were monitored at atomic mass units (AMU) related to the reactant, reaction products and inert gas. Pulses for each AMU were repeated 10 times and averaged to improve the signal-to-noise ratio.
- $^{18}O_2$:Ne = 1:1 and C_2H_6:Ne = 1:1 reaction mixtures were sequentially pulsed by two different pulse valves with different time delays. As in the case of single pulse experiments, pulses were repeated 10 times for each AMU and averaged to improve the signal-to-noise ratio.

3. Results

3.1. Catalyst optimisation

The evolutionary optimisation procedure was carried out up to 10 generations. The development of catalytic performance of the best materials after each generation is shown in Fig. 1. The ethylene yield increases from 9 to 18% under standard conditions. After the seventh generation, no further improvement is observed.

During the optimisation procedure the genetic algorithm has focused on elements, which can be considered as essential for the good performance in the ODHE reaction under the chosen standard conditions (Fig. 2). The elements Cr and Mo have the highest influence on the catalytic performance of the examined complex mixed metal oxides. Other elements like Ca, P, Ga and Zr are less important. Elements of low significance for the ODHE reaction under the conditions examined are La and Cu.

Two different catalytic systems of vanadium-free mixed metal oxides with a certain composition are identified in the best performing materials in the 10th generation. One system consists of Cr and Mo oxides, whereas the other is a complex mixture of Co, Cr, W, and Sn oxides. To the authors' knowledge these mixtures have not yet been reported as active compositions for the ODHE reaction. The compositions of the different systems and their catalytic performance at optimised contact time at 500 °C are listed in Table 2. The ethylene yields achieved in this study are comparable

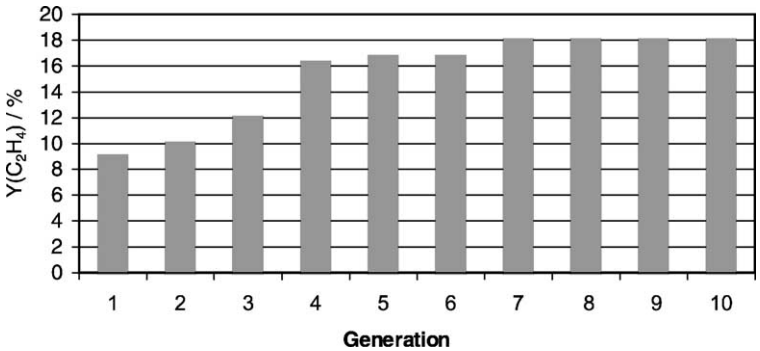

Fig. 1. Evolutionary development of ethylene yield of the best materials after optimising 10 generations of catalytic materials for the ODHE reaction under standard conditions (500 °C; C_2H_6:O_2:Ar = 20:10:70; τ = 0.4 g s/ml; 1 bar).

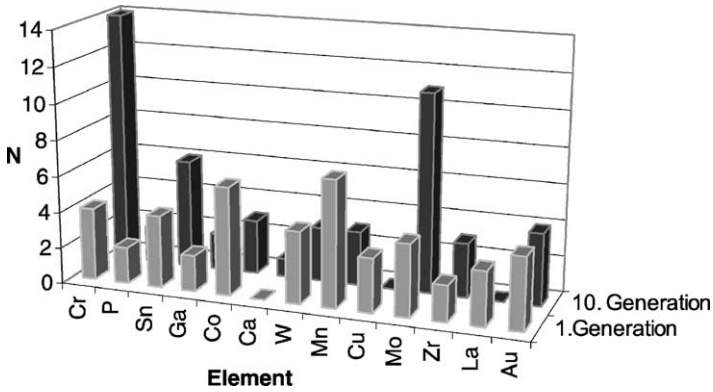

Fig. 2. Appearance frequency of the elements in the 15 best catalytic materials after the 1st and the 10th generation.

to those found for vanadium containing materials under the applied conditions [14–16].

Cr and Mo oxides can be assumed to be active components responsible for a good performance in the ODHE reaction, whereas additional elements like Au and Sn seem to have no influence (Table 2). Cr or Mo oxides alone on α-Al_2O_3 are either less active (Mo) or unselective (Cr) for the ODHE reaction. For the Co/Cr/Sn/W system it is not clear whether only Co and Cr are the active elements or Sn or W are also necessary for a good performance. Co-oxide alone on α-Al_2O_3 exhibits a similar behavior as Cr-oxides whereas a mixture of Sn and W oxides leads to a poorly active material. However, the supported single oxides of Cr, Mo and Co on TiO_2 or ZrO_2 are known to be active materials for the oxidative dehydrogenation of light alkanes [17–21].

The calcination temperature of the materials influences the ODHE performance of the Cr/Mo and Co/Mo/Sn/W systems (Table 3). Calcination at 350 °C results in a better performing material compared to the corresponding material calcined at higher

Table 2
Catalytic performance of different Co/Cr/Sn/W and Cr/Mo systems under optimised conditions for the ODHE reaction after 10 generations of catalyst optimisation

Composition of the active phase on α-Al_2O_3	$X(C_2H_6)$ (%)	$X(O_2)$ (%)	$S(C_2H_4)$ (%)	S (CO_2) (%)	S (CO) (%)	S (CH_4) (%)	Y (C_2H_4) (%)
$Co_{0.280}Cr_{0.398}Sn_{0.158}W_{0.164}O_x$	33	88	63	23	12	2	21
$Co_{0.350}Cr_{0.249}Sn_{0.197}W_{0.205}O_x$[a]	34	81	54	38	8	0	18
$Co_{0.086}Cr_{0.278}Ca_{0.196}Mn_{0.208}P_{0.074}Sn_{0.064}W_{0.093}O_x$	30	88	46	22	22	10	14
$Cr_{0.501}Mo_{0.471}Sn_{0.028}O_x$	32	79	56	7	30	7	18
$Cr_{0.693}Mo_{0.284}Au_{0.023}O_x$	34	90	52	12	31	5	18
$Cr_{0.790}Mo_{0.290}O_x$	32	99	54	12	33	1	17
$Cr_{0.426}Mo_{0.161}Ga_{0.245}Sn_{0.043}Zr_{0.124}O_x$	32	99	53	17	29	1	17
$Cr_{0.601}Mo_{0.246}Au_{0.041}Mn_{0.112}O_x$	32	99	54	12	33	1	17
$Cr_{0.570}Mo_{0.233}Au_{0.038}Ga_{0.109}Zr_{0.049}O_x$	32	98	51	17	31	1	16
CrO_x	16	71	19	58	22	1	3
CoO_x	15	100	18	81	1	0	3
MoO_x	4	15	57	23	17	3	2
$Sn_{0.49}W_{0.51}O_x$	1	4	71	8	20	1	1

Conditions: 500 °C; C_2H_6:O_2:Ar = 20:10:70; τ varied from 0.1 to 1 g s/ml. For comparison the catalytic performance of single oxides of Cr, Mo, Co and a Sn/W are shown. The stoichiometric factors relate to the fraction of the most stable oxide in the active phase.

[a] C_2H_6:O_2 = 1.55.

Table 3
Influence of calcination temperature on catalytic performance of Cr/Mo and Co/Cr/Sn/W catalytic materials

Composition	T (calcination) (°C)	X (C_2H_6) (%)	X (O_2) (%)	S (C_2H_4) (%)	S (CO_2) (%)	S (CO) (%)	Y (C_2H_4) (%)
$Cr_{0.710}Mo_{0.290}O_y$	350	24	51	69	4	27	17
	500	20	61	48	16	34	10
$Co_{0.280}Cr_{0.398}Sn_{0.158}W_{0.164}O_x$	350	14	37	71	19	10	10
	500	9	27	71	18	11	6

S (CH_4) remains always below 2% (500 °C; C_2H_6:O_2:Ar = 20:10:70).

temperatures. The good catalytic performance of the materials calcined at 350 °C was sustained during one week at 500 °C under the reducing reactant atmosphere (C_2H_6:O_2 = 2).

The data shown in Table 3 and Fig. 3 reveal significant differences between the Cr/Mo and Co/Cr/Sn/W systems.

(I) Both systems exhibit comparable ethylene yields and ethane conversions under standard conditions, whereas the Cr/Mo material shows a higher ratio of S (CO):S (CO_2) in contrast to the Co/Cr/Sn/W material.
(II) Ethylene selectivity is almost independent on the ethane conversion over the Co/Cr/Sn/W system, whereas it decreases significantly with conversion over the Cr/Mo system and a vanadium containing reference material (V_2O_5: 15%; MoO_3: 73%; Nb_2O_3: 12%) as shown in Fig. 3.

3.2. Surface and bulk characteristics

The characterisation data were derived for the Cr/Mo and Co/Cr/Sn/W systems calcined at different temperatures. From BET measurements, the surface area is found to be nearly independent on the calcination temperature and ranges between 15 and 20 m^2/g. Dissimilarity of the different calcined materials can be seen for the binding energies (BE) of the electrons,

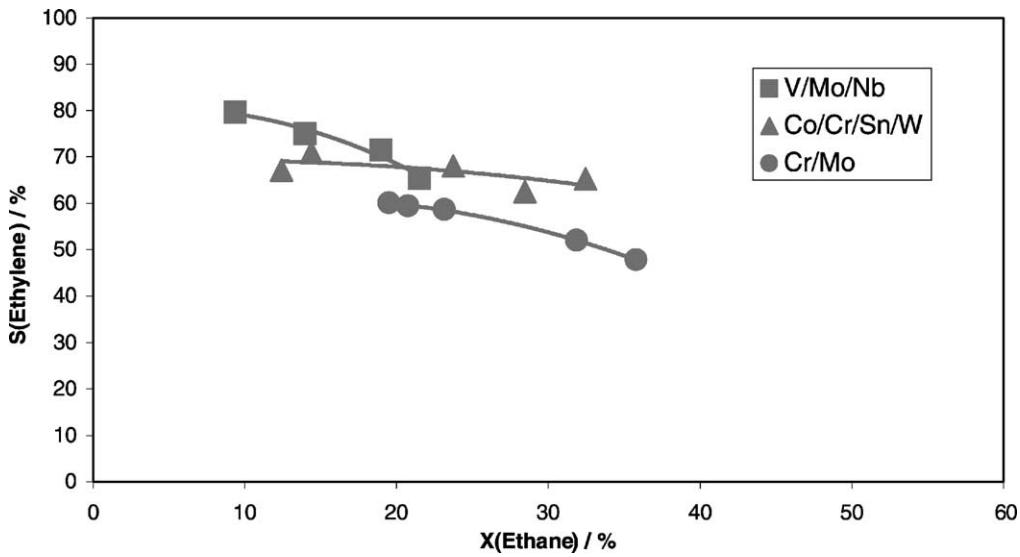

Fig. 3. S (Ethylene) vs. X (Ethane) for the two best catalytic systems from the evolutionary strategy and a vanadium containing material (500 °C; C_2H_6:O_2:Ar = 20:10:70; 1 bar; τ varied from 0.1 to 1 g s/ml).

Table 4
Results from XPS (reference peak C1 284.7 eV) and ICP measurements

Element	Binding energy (eV)				$M_i/\Sigma(M_j)^{XPS}$ (at.%)		$M_i/\Sigma(M_j)^{ICP}$ (at.%)	$M_i/\Sigma(M_j)^{XPS}$ (at.%)		$M_i/\Sigma(M_j)^{ICP}$ (at.%)
	1a	1b	2a	2b	1a	1b	1a + b	2a	2b	2a + b
Mo(VI) 3d	232.4	232.3	–	–	0.2	0.7	0.4	–	–	–
Cr(III) 2p	576.8	576.4	576.8	576.4	0.6	0.2	0.6	0.3	0.4	0.3
Cr(VI) 2p	579.9	578.8	–	–	0.2	0.1	0.6	–	–	0.3
Co(II) 2p	–	–	780.5	781.4	–	–	–	0.3	0.3	0.3
Sn(IV) 3d	–	–	485.3	484.4	–	–	–	0.3	0.3	0.2
W(IV)–W(VI) 4f	–	–	34.7	35.4	–	–	–	0.07	0.05	0.2

Samples: (1a) $Cr_{0.790}Mo_{0.290}O_x$ (calcined at 350 °C); (1b) $Cr_{0.790}Mo_{0.290}O_x$ (calcined at 500 °C); (2a) $Co_{0.280}Cr_{0.398}Sn_{0.158}W_{0.164}O_x$ (calcined at 350 °C); (2b) $Co_{0.280}Cr_{0.398}Sn_{0.158}W_{0.164}O_x$ (calcined at 500 °C).

as determined from XPS and for the amount of the elements determined for the near-surface region by XPS and for the bulk by ICP (Table 4).

For the Cr/Mo material calcined at 350 °C higher Cr 2p binding energies for trivalent Cr(III) and hexavalent Cr(VI) [22,23] have been found in comparison to the corresponding sample calcined at 500 °C. The Mo 3d BE which is nearly independent on the calcination temperature exhibits the typical values of Mo(VI) species [24]. Calcination at a lower temperature leads to a higher surface concentration of both Cr(III) and Cr(VI) oxide species and to a corresponding decrease of the Mo(VI) species concentration on the surface. The surface concentration of the Cr and Mo species shows that the optimal Cr:Mo ratio at the surface is around 4. XRD measurements show that the sample calcined at 350 °C is X-ray amorphous whereas the sample calcined at 500 °C contains crystalline chromium molybdate ($Cr_2(MoO_4)_3$).

In contrast to the Cr/Mo material, only Cr(III) oxide is detected in the Co/Cr/Sn/W composition. XRD measurements of the Co/Cr/Sn/W material calcined at 350 °C reveal only $CoWO_4$ as crystalline phase, the rest of the oxides is located in a X-ray amorphous phase. Since tungsten has a low XPS surface concentration it can be concluded that the part of Co species located in the $CoWO_4$ phase plays a minor role for the performance. The role of Sn is not clear yet.

For the Cr/Mo and Co/Cr/Sn/W systems the active phase is mainly X-ray amorphous. The XRD-patterns of less performing materials exhibit crystalline chromium molybdate or chromium oxide phases. Earlier studies have shown that crystalline chromia is a total oxidation catalyst [25]. For supported catalytic materials it is generally accepted that the spatial isolation of active sites on the catalyst surface is a requirement for selective production of partial oxidation products in ODH reactions [26].

3.3. Mechanistic insights into the ODHE reaction

From the catalytic data in Tables 2 and 3 it can be assumed that steps in the reaction mechanism are different for the Cr/Mo and Co/Cr/Sn/W materials. In order to derive mechanistic insights into the ODHE reaction, heterogeneous steps of the activation of O_2, C_2H_4, C_2H_6 and CO were studied by transient measurements in the TAP reactor.

The interaction of C_2H_6 with Co/Cr/Sn/W and Cr/Mo/Au materials reveals that ethylene, CO and CO_2 were the main products detected at the reactor outlet. In order to check if short-living adsorbed oxygen species take part in the oxidative dehydrogenation of ethane under transient conditions, labelled oxygen ($^{18}O_2$) and ethane were sequentially pulsed over the catalysts at different time intervals. The degree of ethane conversion and product's selectivities did not significantly change when the time interval was varied, indicating that the active oxygen species were stable enough not to be desorbed between two pulses under vacuum. Additionally, only non-labelled oxygen (^{16}O) was observed in $C^{16}O_x$ products (Fig. 4). This means that lattice oxygen of the catalytic material takes part in both the selective oxidative dehydrogenation of ethane towards ethylene and the formation of non-selective reaction products (CO_x). Thus, both the selective and non-selective oxidation of ethane

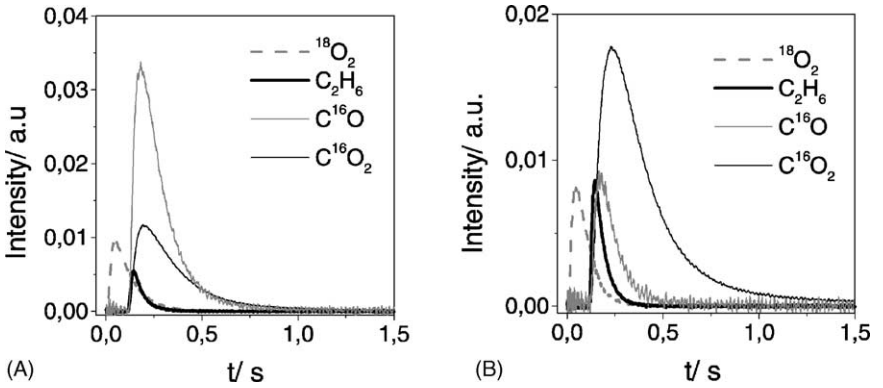

Fig. 4. Transient responses of ethane oxidation reaction. $^{18}O_2$ and ethane were sequentially pulsed at $T = 500\,^{\circ}C$: (A) Cr/Mo/Au-O_x; (B) Co/Cr/Sn/W-O_x; both supported on α-Al_2O_3. (Ethane has been pulsed 0.125 s after the oxygen pulse.)

occurs over the above materials via a Mars–Van Krevelen redox sequence [27], in which ethane reacts with lattice oxygen resulting in anion vacancies followed by oxygen dissociative adsorption and catalyst reoxidation.

The distribution of CO_x products over these materials under transient conditions is the same as observed in the continuous flow experiments; Co/Cr/Sn/W produces more CO_2 than CO in contrast to the Cr/Mo system (Table 2). From the order of the reaction products in the transient responses it can be concluded that over the Co/Cr/Sn/W oxide CO is mainly formed from ethylene followed by its further oxidation to CO_2. This stands in contrast to the Cr/Mo/Au material where CO_2 and CO are parallel products of the secondary oxidation of ethylene. Pulsing of CO_2 alone reveals no interaction with both catalytic materials. Single pulses of ethylene showed that CO and CO_2 are formed in the same sequence as found for the experiments with ethane. From these experiments the following reaction scheme can be suggested (Scheme 1).

Additional experiments on CO pulsing confirmed that the Co/Cr/Sn/W material is much more active for CO oxidation than the Cr/Mo/Au material (Fig. 5A). This may be related to the presence of cobalt and tin oxides in the former material, which have been earlier identified as effective catalysts for CO oxidation [28].

Based on our results on oxygen isotopic exchange (Fig. 5B) we can relate the higher activity of the Co/Cr/Sn/W material towards CO oxidation to its ability to remove easily lattice oxygen.

From the transient experiments, it can be anticipated that for Co/Cr/Sn/W, both CO and ethylene are competing for the same active catalyst sites. This might be the reason for the different dependency of S (ethylene) on X (ethane) shown for the two materials in Fig. 3. The subsequent oxidation of ethylene at high ethane conversions over Co/Cr/Sn/W-O_x is suppressed by the reaction of the formed CO to CO_2 with catalyst lattice oxygen. Therefore, it can be expected that introducing CO into the reactant feed will inhibit the secondary oxidation of ethylene to CO and consequently the ethylene yield might be improved. Preliminary

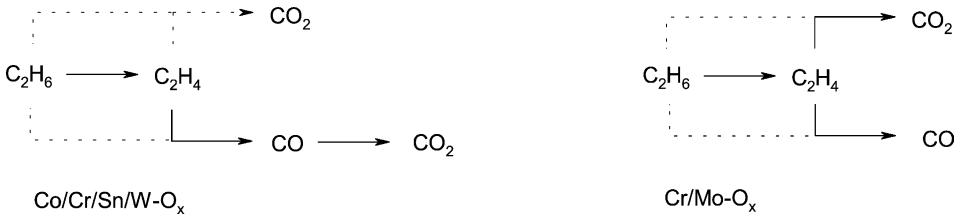

Scheme 1.

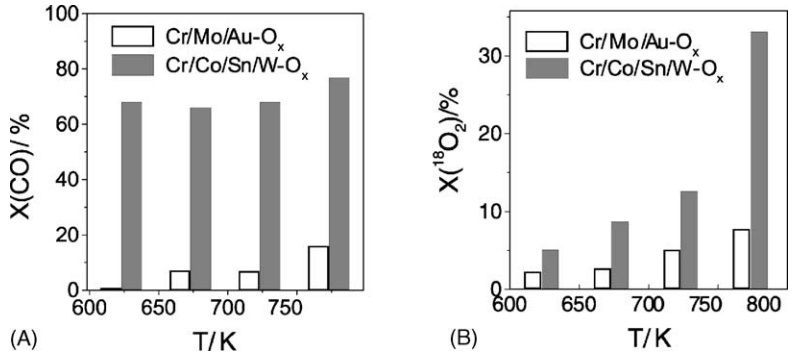

Fig. 5. Activity of Cr/Mo/Au-O_x/α-Al_2O_3 and Co/Cr/Sn/W-O_x/α-Al_2O_3 towards CO oxidation (A) and oxygen isotopic exchange (B) from transient experiments at $T = 500\,^{\circ}C$.

experiments with CO addition to the reaction feed showed that ethylene selectivity and yield are increased for a Co/Cr/Sn/W material when the CO concentration in the feed was changed from 0 to 7.8 vol.%.

4. Conclusions

The application of the evolutionary strategy in search of new catalytic materials for the ODHE reaction excluding vanadium leads to an optimisation of the ethylene yield from 9 to 18% under standard conditions. Two new redox catalytic systems were found comprising oxides of Cr/Mo and Co/Cr/Sn/W. By optimizing the reaction conditions the yield can be further increased up to $Y = 21\%$ over $Co_{0.280}Cr_{0.398}Sn_{0.158}W_{0.164}O_x$ (500 °C; C_2H_6:O_2:Ar = 20:10:70; $\tau = 1$ g s/ml) and it is comparable to those found for vanadium-based ODHE catalysts. For the two systems, XPS and XRD measurements revealed that the active phase (Cr/Mo or Co/Cr/Sn/(W) oxide) is located in the X-ray amorphous part of the material.

From transient experiments it can be concluded that the Co/Cr/Sn/W material is more active for the further reaction of CO to CO_2, whereas CO competes with ethylene for the same active sites. This leads to: (i) a higher selectivity towards CO_2; and (ii) a higher ethylene selectivity at high ethane conversions compared to the Cr/Mo system.

It can be assumed that the performance of the two systems is improved by increasing the dispersion of the mixed Cr/Mo and Co/Cr/Sn/(W) oxides. This can be achieved by applying new preparation methods leading to a high surface area or support materials with a high surface area. Another possibility for materials with increased catalytic performance might be the use of porous MoO_3 as a support for highly dispersed Cr oxide for the Cr/Mo system and high surface SnO_2 or WO_3 for the deposition of Co/Cr oxides for the Co/Cr/Sn/W system.

Acknowledgements

The authors thank Dipl. Chem. L. Cholinska for parallel catalyst testing, Dipl. Chem. L. Mader for transient studies, Dr. M. Schneider for XRD analysis, Dr. J. Radnik for XPS measurements. The work was supported by the European commission within its fifth Framework Program: *COMBICAT*, Project no. GRD-CT1999-10696, title “Catalyst design and optimisation by fast combinatorial analysis” as well as the state of Berlin and BMBF.

References

[1] M. Baerns, O.V. Buyevskaya, Catal. Today 45 (1998) 13.
[2] M.A. Banares, Catal. Today 51 (1999) 319.
[3] M. Huff, L.D. Schmidt, J. Phys. Chem. 97 (1993) 11815.
[4] A.S. Bodke, D. Henning, L.D. Schmidt, S.S. Bharadwaj, J.J. Maj, J. Siddall, J. Catal. 191 (2000) 62.
[5] S.A.R. Mulla, O.V. Buyevskaya, M. Baerns, J. Catal. 197 (2001) 43.
[6] E.M. Thorsteinson, T.P. Wilson, F.G. Young, P.H. Kasa, J. Catal. 52 (1978) 116.

[7] O.V. Buyevskaya, D. Wolf, M. Baerns, Catal. Today 62 (2000) 91.
[8] D. Wolf, O.V. Buyevskaya, M. Baerns, Appl. Catal. A 200 (2000) 63.
[9] O.V. Buyevskaya, A. Brückner, E.V. Kondratenko, D. Wolf, M. Baerns, Catal. Today 67 (2001) 369.
[10] O.V. Buyevskaya, M. Baerns, Catalysis 16 (2002) 155.
[11] F. Cavani, F. Trifirò, Catal. Today 51 (1999) 561.
[12] I. Hahndorf, O.V. Buyevskaya, M. Langpape, G. Grubert, S. Kolf, E. Guillon, M. Baerns, Chem. Eng. J. 89 (2002) 119.
[13] J.T. Gleaves, G.S. Yablonskii, P. Phanawadee, Y. Schuurman, Appl. Catal. 160 (1997) 55.
[14] T. Blasco, A. Galli, J.M. López Nieto, F. Trifiro, J. Catal. 169 (1997) 203.
[15] Q. Zhang, Y. Wang, Y. Ohishi, T. Shishido, K. Takehira, J. Catal. 202 (2001) 308.
[16] B. Solsona, T. Blasco, J.M. López Nieto, M.L. Peña, F. Rey, A. Vidal-Moya, J. Catal. 203 (2001) 443.
[17] Y. Brik, M. Kacimi, M. Ziyad, F. Bozon-Verduraz, J. Catal. 202 (2001) 118.
[18] A. Aadane, M. Kacimi, M. Ziyad, Catal. Lett. 73 (2001) 47.
[19] J. El-Idrissi, M. Kacimi, F. Bozon-Verduraz, M. Ziyad, Catal. Lett. 56 (1998) 221.
[20] M. Loukah, G. Coudurier, J.C. Vedrine, M. Ziyad, Micropor. Mater. 4 (1995) 345.
[21] K. Chen, S. Xie, A.T. Bell, E. Iglesia, J. Catal. 198 (2001) 232.
[22] S. Wang, K. Murata, T. Hayakawa, S. Hamakawa, K. Suzuki, Catal. Lett. 73 (2001) 107.
[23] B. Solsona, J.M. López Nieto, M. Alcantara-Rodriguez, E. Rodriguez-Castellon, A. Jimenez-Lopez, J. Mol. Catal. A: Chem. 153 (2000) 199.
[24] R.B. Watson, U.S. Ozkan, J. Catal. 191 (2000) 12.
[25] M. Loukah, G. Coudirier, J.C. Vedrine, in: P. Ruíz, B. Delmon (Eds.), New Developments in Selective Oxidation by Heterogeneous Catalysts, vol. 72, 1992, p. 191.
[26] R.K. Grasselli, Topics Catal. 9 (2001) 93.
[27] P. Mars, D.W. Van Krevelen, Chem. Eng. Sci. 3 (1954) 41.
[28] G.K. Boreskov, Heterogeneous Catalysis, Nauka, Moscow, 1984.